Adv. Polar Upper Atmos. Res., 13, 48–56, 1999

# EISCAT SVALBARD RADAR-DERIVED ATMOSPHERIC TIDAL FEATURES IN THE LOWER THERMOSPHERE AS COMPARED WITH THE NUMERICAL MODELING ATM2

Takehiko Aso[1], Anthony VAN EYKEN[2] and Phil J. S. WILLIAMS[3]

[1] *National Institute of Polar Research, Kaga 1-chome, Itabashi-ku, Tokyo 173-8515*
[2] *EISCAT Scientific Association, Longyearbyen, Norway*
[3] *The Department of Physics, The University of Wales, Aberystwyth, Wales, U.K.*

***Abstract:*** The EISCAT Svalbard radar (ESR) has obtained neutral wind field data down to 90 km altitude in two period runs in August 1998. This has been rendered possible by successful elimination of ground clutter echoes by the ESR staff. Features of the obtained tidal components are then comparatively studied with the ATM2 (Atmospheric Tidal Modeling Version 2) steady tidal model which assumes climatological background zonal flow. It is found that the results are fairly consistent with theoretical predictions that the diurnal component is almost evanescent with some indication of propagating characteristics, and that the semi-diurnal one is dominated by short vertical wavelength higher order mode prevalent at higher latitudes. The ter-diurnal component is also not in contradiction with non-linear interaction theory. Convincing delineation of these behaviors, however, awaits further study on the zonal wave number characteristics of relevant waves by longitudinal network collaborations.

## 1. Introduction

The EISCAT Svalbard radar (78.2°N, 16.1°E) has become in operation in 1977 and some preliminary results have been published as to the sounding of upper atmosphere region above 115 km (WANNBERG *et al.*, 1997). Since the upgrade of transmitter power to 1 MW in December 1997, a ground clutter problem has been tackled and echo returns down to 90 km altitude have become available for the study of dynamics in the mesopause region at polar latitudes. In August 1998, a tidal dynamics run was carried out and 70 hours data during the Test run on 11–14 August (VAN EYKEN *et al.*, 1999) and 51 hours data during the CP (Common Program) run on 17–19 August are obtained for the altitude region from 93 to 120 km. In this paper, preliminary analyses are carried out to be compared with the steady modeling of atmospheric tides by the ATM2 (Atmospheric Tidal Modeling Version 2) developed in early 1980's by Aso *et al.* (1987).

## 2. Observation

The EISCAT Svalbard radar is located at Longyearbyen, Svalbard (78.2°N, 16.1°E). It operates at UHF frequencies of 500 MHz with a peak power of 1 MW. In the observations, the antenna was pointing to its local magnetic zenith which has the

inclination of 82° and declination of 2°. A new GUP3 coding was used to explore the altitude from 90 to 550 km, and here use is made of the ion drift velocity at the interval of 1 min or 2 min in time and 3 km between 93 and 120 km altitude. A field-aligned ion velocity is assumed to be representative of neutral wind projected to the geomagnetic lines of force in that below 120 km $\nu_{in} > \Omega_i$, *i.e.*, ion-neutral collision frequency $\nu_{in}$ dominates the ion gyrofrequency $\Omega_i$ (BREKKE, 1997) and parallel electric field is small. If we focus on the long period waves, the wind field is mainly horizontal (vertical component is two or three orders of magnitude smaller). So the line-of-sight velocity divided by cos 82° is assumed to represent meridional wind component of pertinent neutral motion. In the GUISDAP (Grand Unified Incoherent Scatter Design and Analysis Package, 1994) analysis, positive sign refers to the velocity towards the radar contrary to the NCAR convention, hence positive values refer to northward. All measured velocities at 1 min or 2 min intervals are averaged over ±30 min with data of more than three standard deviations from the average being eliminated, and time series in steps of 0.25 hour are provided for further tidal analysis. At high latitudes, auroral disturbances are expected to cause changes in neutral wind field. During the radar run, magnetic activity became enhanced three times, at 2330 UT on August 11 and 12, and 1500 UT on August 14. But corresponding changes in ion drift velocity occurred only above about 150 km. The geomagnetic activity effect on mesopause neutral wind is still worthy of further study (*e.g.* WAND, 1983; JOHNSON and LUHMANN, 1985) and will be discussed elsewhere.

## 3. Tidal Analysis

Figures 1a and 1b show the frequency spectra *versus* altitude for the Test and CP runs, respectively. As the data points are unevenly sampled, the Lomb method is used to obtain periodgrams at each height (PRESS *et al.*, 1992). In the figure, vertical axis is in unit of cycles/day and 1.0 and 2.0 correspond to diurnal and semi-diurnal components, respectively. Shaded contour represents spectral power. In the Test run (a), it is seen that the diurnal component dominates at higher altitudes, whereas the semi-diurnal components appear at most of the altitudes. Also, signatures of ter-diurnal and quatra-diurnal components and some other short period waves like 2.5 cpd (~10 hr) are apparent. The 10.4 h component corresponds to the period of a first anti-symmetric normal mode of zonal wavenumber $s = 1$ with equivalent depth of $\gamma H \cong 10$ km where $\gamma$ is the ratio of specific heats and $H$ is a scale height (FORBES *et al.*, 1999).

For the CP run in Fig. 1b, a semi-diurnal component, not exactly 12 hr at some heights, is less dominant at higher altitudes where a diurnal component predominates. A ter-diurnal component is also traced as in Fig. 1a.

Now, we extract the amplitude and phase of relevant tidal components by fitting mean plus diurnal, semi-diurnal and ter-diurnal sinusoidal components to time series at each height. Linear least square fitting gives uncertainty in cosine and sine terms of each harmonic components. Uncertainties in amplitude and phase are then estimated to be mostly less than 1 m/s and 1 hr respectively, and hence are not indicated in the figure. Figure 2 indicates the amplitude by solid lines and the phase by dashed lines of the diurnal component for Test and CP runs which are identified by solid circle and

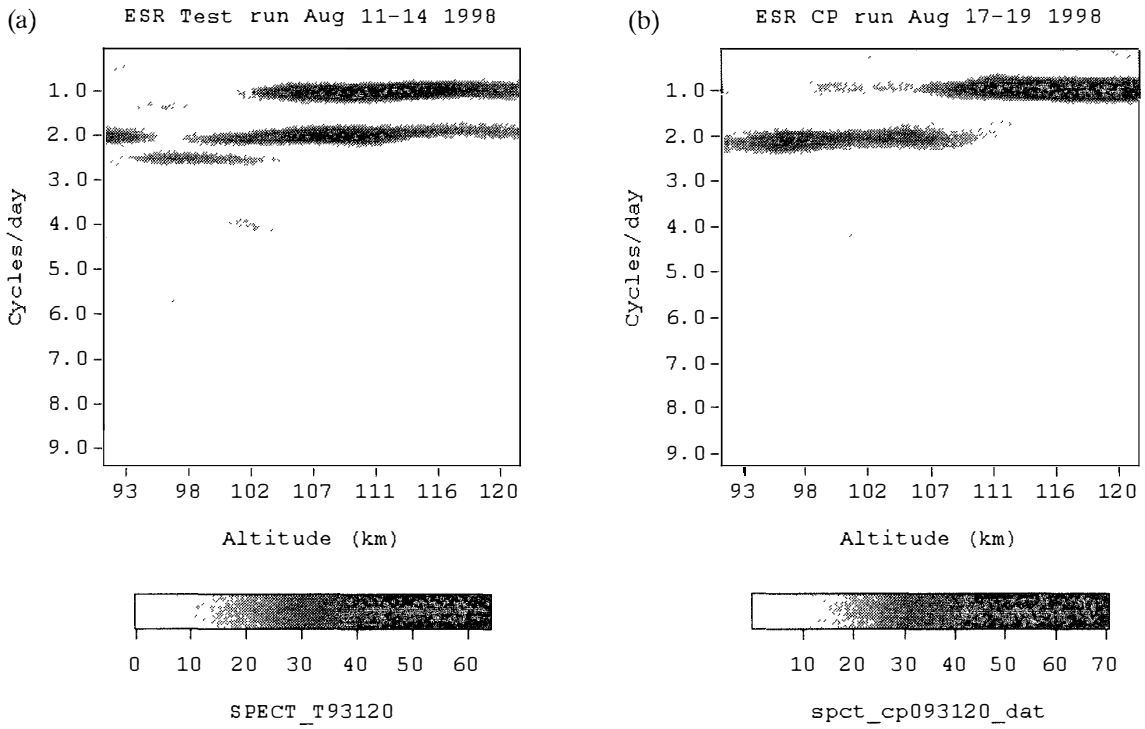


*Fig. 1. Spectra versus altitude of the meridional wind observed by the EISCAT Svalbard radar during the Test (a) and CP (b) runs in August.*

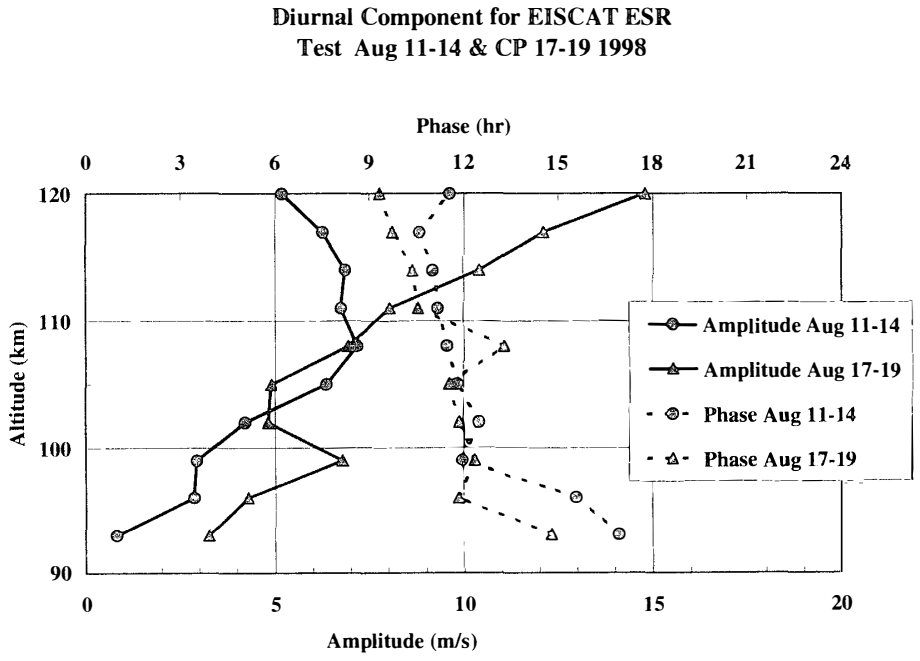


*Fig. 2. Altitude profiles of the amplitude (solid line) and phase (dashed line) of 24-hr component for the Test (circle) and CP (triangle) periods.*

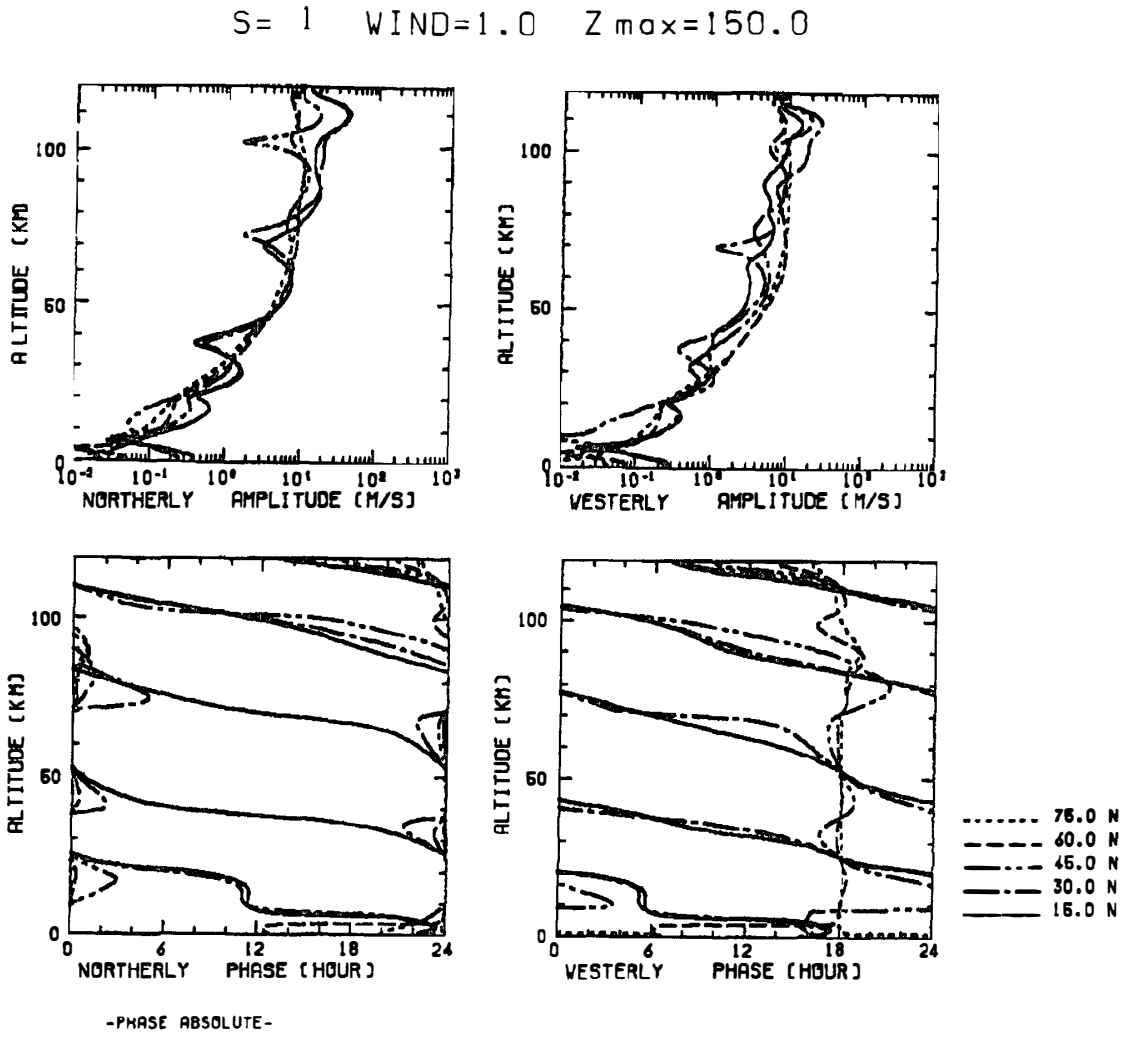


*Fig. 3. Numerical profiles of the northerly (left) and westerly (right) components of diurnal tide for the June solstice wind condition by the ATM2 modeling. Latitudes are 15° (solid), 30° (dashed-dot), 45° (dashed-double-dot), 60° (dashed) and 75° (dotted) in the Northern Hemisphere.*

triangle symbols, respectively. Phase is in UT hours. As the local time is 1 hr ahead of the universal time (UT), phase values in LT are UT+1 hr. Amplitude is lager at higher altitudes for CP period, consistent with spectral analysis in Fig. 1. As for the phase, it shows almost evanescent nature with a little bit of mixed propagating mode. The northward maximum around 1200 LT is very much consistent with theoretical predictions by the classical theory and by the ATM2 modeling result shown in Fig. 3. The model solves the coupled partial differential equations for the velocity vector and temperature perturbations in the atmosphere with latitudinal temperature gradient and background mean zonal flow. Also included are a transport of heat and momentum by molecular and eddy diffusion, Newtonian cooling, parameterized gravity wave drag (Forbes *et al.*, 1991) as a possible dissipation effective on short-vertical wavelength diurnal modes, and also horizontal diffusion for computational stability. In the modeling, resolutions in altitude and latitude are 250 m and 2.5°, respectively and background

wind at June solstice is assumed based on the CIRA86 wind model. It is evident that the diurnal tide is propagating at latitudes equatorward of 30° latitude where the inertial period is longer than 24 hr while at higher latitudes, the evanescent mode due to (1, −2) forcing becomes dominant which represents fairly stable phase around 1200 and 1800 LT for northward and eastward component, respectively. In between, *e.g.*, at 45°N at lower heights and at 60°N above 90 km, phase rotation with respect to altitude is indicative of mixtures of evanescent and propagating modes. The present numerical modeling for the effect of background zonal wind on the non-migrating diurnal tide suggests the penetration of propagating component to higher latitudes (EKANAYAKE *et al.*, 1997). This is due to the increased Doppler shifted wave frequency of the westward propagating component in the strong westerly wind regime in the winter hemisphere and *vice versa* as in

$$\tilde{\sigma}=\sigma+\frac{s\cdot V}{a\cdot\sin\theta},$$

where $a$ is the earth radius, $V$, background zonal wind, and $\theta$, colatitude. A slight phase slope envisaged in Fig. 2 is interpreted as a mixture of propagating non-migrating component to evanescent modes.

The semi-diurnal period component is shown in Fig. 4. Amplitude ranges around 5 m/s corresponding to 35 m/s (1/cos 82° ≅ 7) of meridional wind. Amplitude profiles are not inconsistent with theoretical prediction by the ATM2 model which is shown in Fig. 5. Phase slope signifies rather short vertical wavelength of 30–35 km which is short compared with higher order (2, 4) (50 km) or even (2, 5) (40 km) modes. The modeling reveals the dominance of a fairly short vertical wavelength above 90 km at polar latitudes. At 75°N, the phase undergoes rapid excursion above 90 km corre-

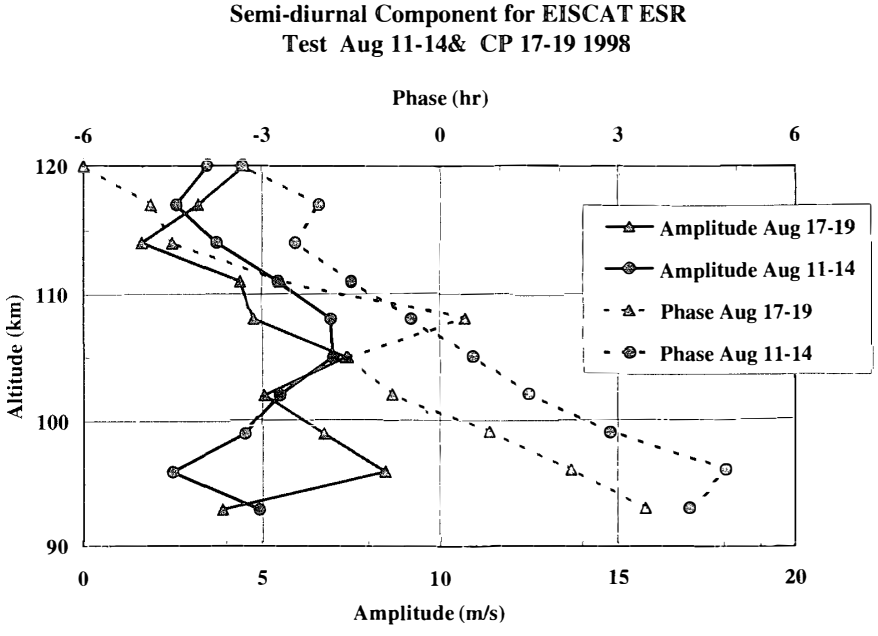


*Fig. 4. As in Fig. 2 except for the 12-hr component.*

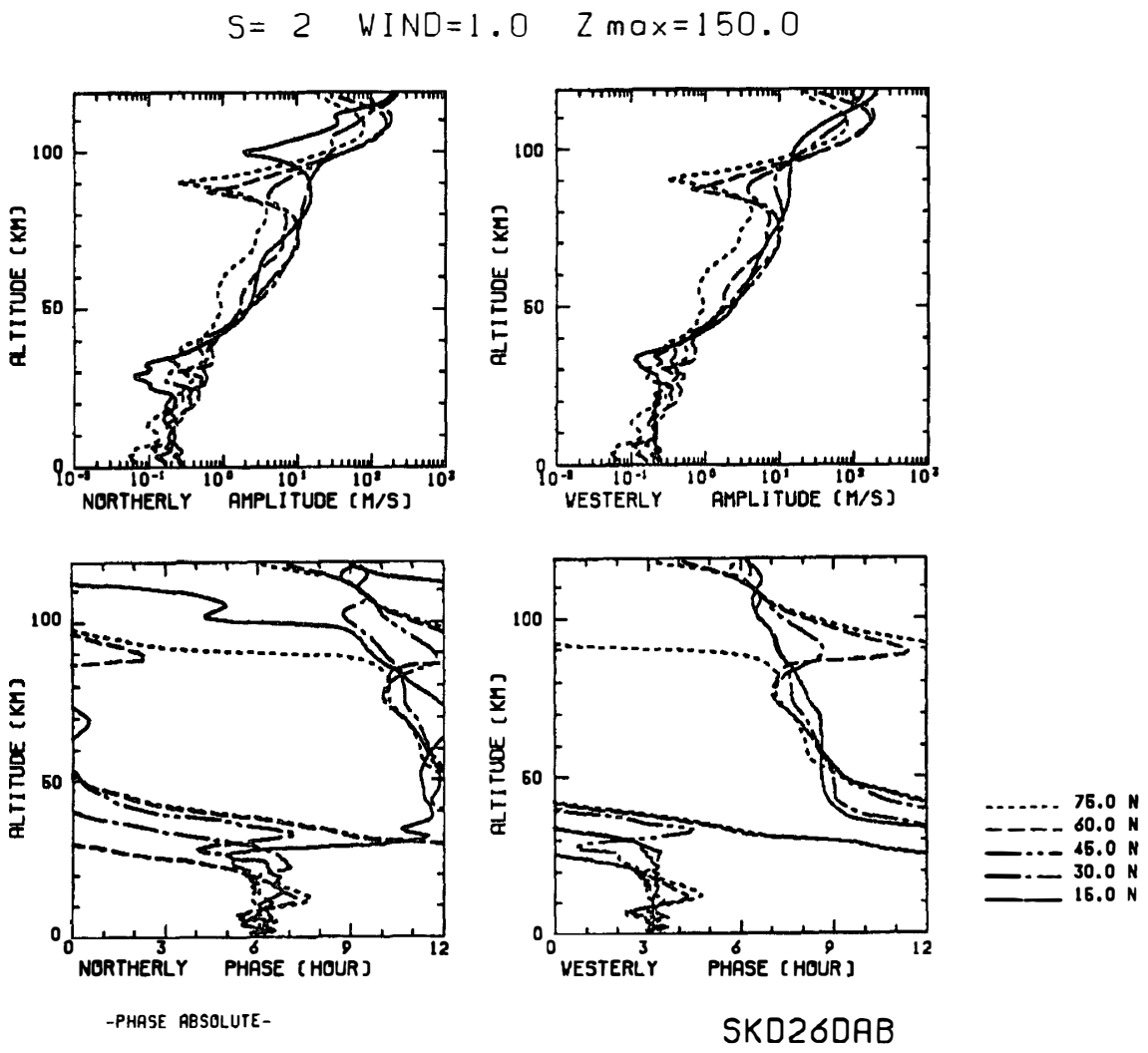


*Fig. 5. As in Fig. 3 except for the semi-diurnal tide.*

sponding to the amplitude minimum. As has been shown by LINDZEN and HONG (1974) and by ASO *et al.* (1981) the semi-diurnal tide is more influenced by the background wind. Higher order modes thus excited predominate at higher latitudes, giving rise to shorter vertical wavelength characteristics.

Figure 5 suggests the northward phase of 0500 LT at about 100 km height which is slightly different from observed values of 0000–0300 LT. Different wind model gives some difference, and absolute agreement in phase in this short-vertical region is not to be expected. Also, FORBES *et al.* (1995) discovered the dominant $s=1$ westward moving semi-diurnal component in summer time by the South Pole meteor radar by identifying the zonal wavenumber of the relevant oscillation. This is fairly consistent with the intuition that $s=2$ wind component should vanish at the pole. The origin of this component is not clear though the prediction of the nonlinear interaction of migrating semi-diurnal component with stationary $s=1$ planetary wave was studied numerically by MIYAHARA and MIYOSHI (1997). The consistency of the observed steep phase slope by ESR should further be investigated by identifying pertinent zonal wavenumber.

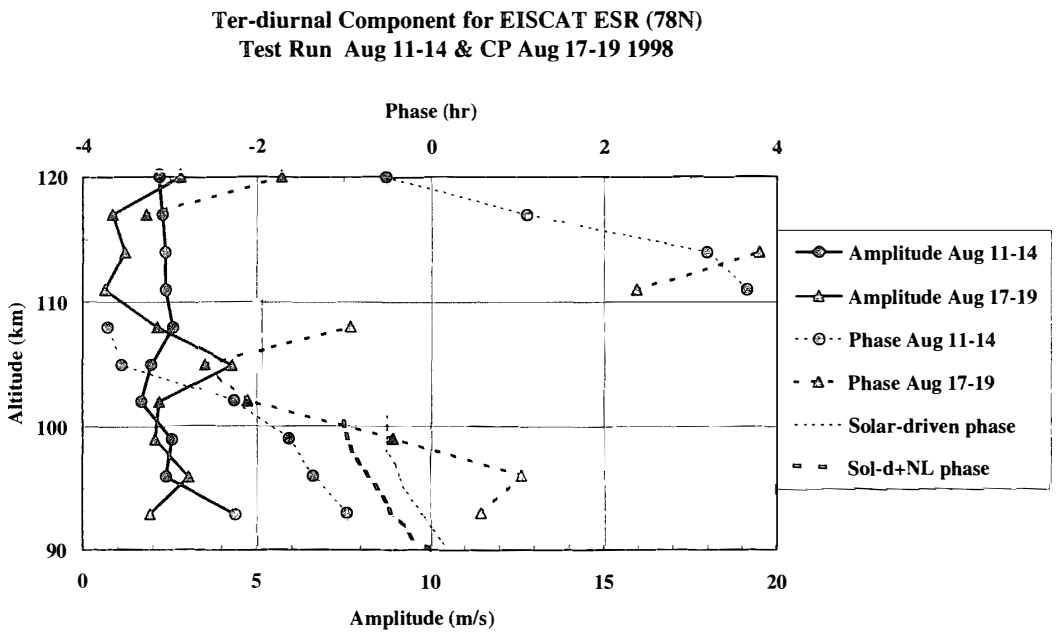


*Fig. 6. As in Fig. 2 except for the 8-hr component. Theoretical predictions are for 47°N latitude by* TEITELBAUM *et al. (1989).*

Figure 6 shows the result for ter-diurnal component as compared with the theoretical prediction by TEITELBAUM *et al.* (1989). Theoretical values of phase at 47°N are given for solar-driven components by the third harmonic of insolation absorption with and without the effect of non-linear coupling of migrating diurnal and semi-diurnal component by the advection term. The phase is shifted by 2 hr to be compared with the northward component. Latitudinal phase variation between 47°N and 79°N in summer dose not differ too much and observed phase values are, by and large, consistent with the theory below 100 km. Equivalent depths of ter-diurnal tide are 12.9, 7.7, 5.1 km···etc and its vertical wavelength is fairly large, while the observed one is very short in some case. These are also issues to be studied by relevant numerical model.

## 4. Discussions

A first attempt to derive tidal features of the lower thermospheric regions by the EISCAT Svalbard radar is an impetus to extend coordinated observation of lower thermosphere tides at polar region. This was made possible by the ESR staff's efforts to reduce the ground clutter which precluded the sounding of lower *E* region.

Two runs of 2–3 days duration thus analysed have given a general view on the meridional wind variations of tidal periods in the altitude range of 90–120 km. It is found that the diurnal component is rather stable in phase which is consistent with dominant evanescent mode in the polar latitude summer time and is a common feature indicated in the atmosphere tidal modeling. Also, a phase tilt suggests a mixture of non-migrating tides. Further evidence, however, requires the zonal wavenumber information. As for the semi-diurnal component, phase excursion is fairly rapid which is consistent with our numerical model. This short vertical wavelength characteristic

renders the averaged tidal amplitude smaller. Possible 12 hr period oscillations as the pseudo-tide due to tidal modulation of gravity wave momentum flux in the mesopause region (WALTERSCHEID *et al.*, 1986) or inertial period oscillation close to 12 hr are to be paid some attention with regard to interpretation of this component. The summertime $s=1$ semi-diurnal component as observed at the South-Pole is however not resolved in the present analysis. Hence, zonal wavenumber is really an important parameter along with latitudinal structure in this highly variable wave regime. The ter-diurnal component observed in ESR data is rather rudimentary though the steeper phase gradient indicative of nonlinear coupling is not inconsistent with our result. MANSON and MEEK (1986) reported that ter-diurnal amplitude is growing larger above 100 km and that its phase gradient is large and irregular in summer which is also consistent with our findings. They also noted longer vertical wavelength in winter. Thus global longitudinal collaborations between observing sites at polar latitude are urgent issues to resolve these structured tidal characteristics.

## 5. Conclusion

A two-period tidal observation run was carried out and preliminary signatures of atmospheric tidal oscillation observed by the EISCAT Svalbard radar have been caught a glimpse. Basically, they are consistent with the steady tidal modeling. It is, however, envisaged that further sophistications both in observation and theory are needed to fully or quantitatively understand the physical process, *e.g.*, local effects at auroral latitudes and dynamical coupling and nonlinear interactions in the whole polar middle atmosphere.

Longitudinal study based on combinations of radars along the arctic circle, and arctic/antarctic distinction study between two polar hemispheric regions are thus a key to our goal.

## Acknowledgments

The authors are grateful to the Director and staff of the EISCAT Scientific Association, an international association supported by Finland, France, Germany, Japan, Norway, Sweden, and United Kingdom for operating the facility and supplying the data. We also wish to thank S. Buchert for provision of analysis and data transfer.

### References

ASO, T., NONOYAMA, T. and KATO, S. (1981): Numerical simulation of semidiurnal atmospheric tides. J. Geophys. Res., **86**, 11388–11400.

ASO, T., ITO, S. and KATO, S. (1987): Background wind effect on the diurnal tide in the middle atmosphere. J. Geomagn. Geoelectr., **39**, 297–305.

BREKKE, A. (1997): Physics of the Upper Polar Atmosphere. Chichester, J. Wiley, Chapter 7, 313–388.

EKANAYAKE, E.M.P., ASO, T. and MIYAHARA, S. (1997): Background wind effect on propagation of nonmigrating diurnal tides in the middle atmosphere. J. Atmos. Solar-Terr. Phys., **59**, 401–429.

FORBES, J.M., GU, J. and MIYAHARA, S. (1991): On the interaction between gravity waves and the diurnal propagating tide. Planet. Space Sci., **39**, 1249–1257.

FORBES, J.M., MAKAROV, N.A. and PORTHNYAGIN, Y.I. (1995): First results from the meteor radar at South Pole: A large 12-hour oscillation with zonal wavenumber one. Geophys. Res. Lett., **22**, 3247–3250.

FORBES, J.M., PALO, S.E., ZHANG, X., PORTNYAGIN, Y.I., MAKAROV, N.A. and MERZLYAKOV, E.G. (1999): Lamb waves in the lower thermosphere: Observation evidence and global consequences. J. Geophys. Res. (in press).

GUISDAP (1994): Workshop report, Rutherford Appleton Laboratory, 9–13 May.

JOHNSON, R.M. and LUHMANN, J.G. (1985): High-latitude mesopause neutral winds and geomagnetic activity: A cross-correlation analysis. J. Geophys. Res., **90**, 8501–8506.

LINDZEN, R.S. and HONG, S-S. (1974): Effects of mean winds and horizontal temperature gradients on solar and lunar semidiurnal tides in the atmosphere. J. Atmos. Sci., **31**, 1421–1446.

MANSON, A.H. and MEEK, C.E. (1986): Dynamics of the middle atmosphere at Saskatoon (52°N, 107°W): A spectral study during 1981, 1982. J. Atmos. Terr. Phys., **48**, 1039–1055.

MIYAHARA, S. and MIYOSHI, Y. (1997): Migrating and non-migrating atmospheric tides simulated by a middle atmosphere general circulation model. Adv. Space Res., **20**, 1201–1207.

PRESS, W.H., TEUKOLSKY, S.A., VETTERLING, W.T. and FLANNERY, B.P. (1992): Numerical Recipes in FORTRAN. Cambridge, Cambridge Univ. Press, 963 p.

TEITELBAUM, H., VIAL, F., MAONSON, A.H., GIRALDEZ, R. and MASSEHENF, M. (1989): Non-Linear interaction between diurnal and semidiurnal tides: Terdiurnal and diurnal secondary waves. J. Atmos. Terr. Phys., **51**, 627–634.

VAN EYKEN A.P., WILLIAMS, P.J.S., KUNITAKE, M. and BUCHERT, S. (1999): First *E*-region observations of tides in the lower thermosphere using the EISCAT Svalbard Radar. submitted to Geophys. Res. Lett.

WAND, R.H. (1983): Geomagnetic activity effects on semidiurnal winds in the lower thermosphere. J. Geophys. Res., **88**, 9243–9248.

WALTERSCHEID, R.L., SIVJEE, G.G., SCHUBERT, G. and HAMWEY, R.M. (1986): Large amplitude semidiurnal temperature variations in the polar mesopause: evidence of a pseudotide. Nature, **324**, 347–349.

WANNBERG, U.G., WOLF, I., VANHAINEN, L.-G., KOSKENNIEMI, K., ROTTGER, J., POSTILA, M., MARKKANEN, J., JACOBSEN, R., STENBERG, A., LARSEN, R., ELIASSEN, S., HECK, S. and HUUSKONEN, A. (1997): The EISCAT Svalbard radar, a case study in modern incoherent scatter radar system design. Radio Sci., **32**, 2283–2307.

*(Received March 1, 1999; Revised manuscript accepted May 18, 1999)*